chemistry

MDPI

Communication

Synthesis of Selenium-Based Small Molecules Inspired by CNS-Targeting Psychotropic Drugs and Mediators

Giovanni Ribaudo [1,*,†], Davide Zeppilli [2,†], Alberto Ongaro [3], Marco Bortoli [4], Giuseppe Zagotto [3] and Laura Orian [2,*]

[1] Dipartimento di Medicina Molecolare e Traslazionale, Università degli Studi di Brescia, Viale Europa 11, 25123 Brescia, Italy
[2] Dipartimento di Scienze Chimiche, Università degli Studi di Padova, Via Marzolo 1, 35131 Padova, Italy; davide.zeppilli@studenti.unipd.it
[3] Dipartimento di Scienze del Farmaco, Università degli Studi di Padova, Via Marzolo 5, 35131 Padova, Italy; alberto.ongaro@unipd.it (A.O.); giuseppe.zagotto@unipd.it (G.Z.)
[4] Department of Chemistry and Hylleraas Centre for Quantum Molecular Sciences, University of Oslo, 0315 Oslo, Norway; marco.bortoli@kjemi.uio.no
* Correspondence: giovanni.ribaudo@unibs.it (G.R.); laura.orian@unipd.it (L.O.); Tel.: +39-030-3717419 (G.R.); +39-049-8275140 (L.O.)
† These authors contributed equally to this work.

Abstract: Due to its endogenously high oxygen consumption, the central nervous system (CNS) is vulnerable to oxidative stress conditions. Notably, the activity of several CNS-targeting compounds, such as antidepressant and hypnotic drugs, or endogenous mediators, such as melatonin, is indeed linked to their ability of mitigating oxidative stress. In this work, we report the synthesis of two organoselenium compounds of which the structure was inspired by CNS-targeting psychotropic drugs (zolpidem and fluoxetine) and an endogenous mediator (melatonin). The molecules were designed with the aim of combining the ROS-scavenging properties, which were already assessed for the parent compounds, with a secondary antioxidant action, a glutathione peroxidase (GPx) mimic role empowered by the presence of selenium. The compounds were obtained through a facile three-step synthesis and were predicted by computational tools to passively permeate through the blood–brain barrier and to efficiently bind to the GABA A receptor, the macromolecular target of zolpidem. Of note, the designed synthetic pathway enables the production of several other derivatives through minor modifications of the scheme, paving the way for structure–activity relationship studies.

Keywords: antioxidant; CNS; glutathione peroxidase; melatonin; selenium; zolpidem

Citation: Ribaudo, G.; Zeppilli, D.; Ongaro, A.; Bortoli, M.; Zagotto, G.; Orian, L. Synthesis of Selenium-Based Small Molecules Inspired by CNS-Targeting Psychotropic Drugs and Mediators. *Chemistry* **2023**, *5*, 1488–1496. https://doi.org/10.3390/chemistry5030101

Academic Editor: George O'Doherty

Received: 21 May 2023
Revised: 18 June 2023
Accepted: 22 June 2023
Published: 27 June 2023

1. Introduction

An intracellular equilibrium between antioxidant and pro-oxidant species, also defined as cellular redox balance, exists in living beings. Its alteration with an excess of harmful free radicals leads to oxidative stress [1], eventually resulting in cardiovascular diseases [2] and some types of cancer [3] and in pathological conditions that may also affect the central nervous system (CNS), e.g., neurodegenerative disorders [4], as well as mood disorders [5] and schizophrenia [6].

Endogenous antioxidants, including enzymes such as superoxide dismutase (SOD) [7], glutathione peroxidase (GPx) [8,9], and catalase [10], can mitigate oxidative stress by inhibiting radical-promoted oxidation processes [11]. On the other hand, exogenous antioxidants comprehend natural substances acting as free radical scavengers often constituted by dietary compounds. Flavonoids, carotenoids, omega-3 fatty acids, ginkgolides and bilobalide, melatonin, which is also endogenous, and ascorbic acid represent some examples [12–15].

CNS is particularly vulnerable to oxidative stress, due to its high oxygen consumption. It is noteworthy that the action of some drugs used for the treatment of CNS diseases, such

as the antidepressant fluoxetine and the hypnotic zolpidem, was linked to their ability to mitigate oxidative stress [14,16–19].

In this work, we designed, synthesized, and characterized two new molecules (**1**–**2**) that include some structural motifs from CNS drugs and natural compounds showing ROS scavenging properties. For the benzimidazole scaffold, we took inspiration from the structure of zolpidem (**3**) and melatonin (**4**); the ethyl linker is common to melatonin (**4**) and fluoxetine (**5**); finally, we introduced a selenium center to potentially enhance the antioxidant properties (Scheme 1) in light of its capacity to reduce hydroperoxides and enable a GPx-like activity [17,20].

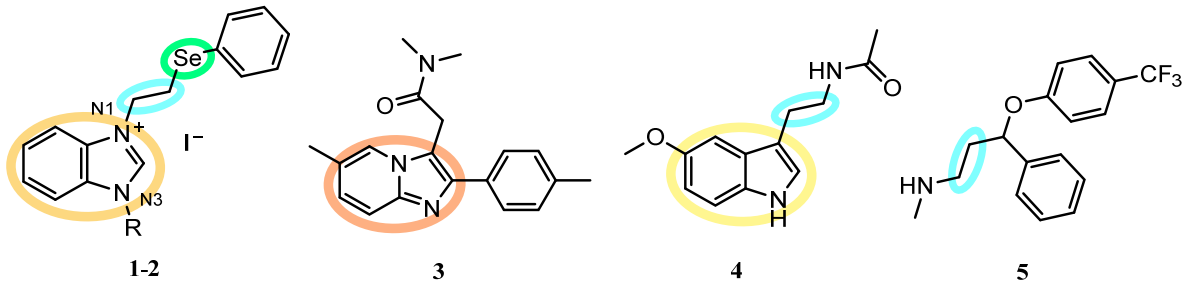

1-2 **3** **4** **5**

Scheme 1. Chemical structures of compounds **1**–**2**, zolpidem (**3**), melatonin (**4**), and fluoxetine (**5**). Recurring chemical motifs were highlighted with similar colors in the scheme.

2. Results and Discussion

With this work, we aimed at paving the way, from a synthetic point of view, for the preparation of a new generation of tandem-antioxidants, inspired by active ROS scavengers chosen among CNS-targeting psychotropic drugs, i.e., zolpidem and fluoxetine, and endogenous mediators, i.e., melatonin, to which a GPx mimic selenium center was added. These compounds were conceived with the idea of combining a primary antioxidant action, connecting the ROS scavenging properties with a secondary antioxidant action, related to the presence of the chalcogen center and the GPx molecular mimic role [20].

The scaffold of **1** and **2** consists of a disubstituted benzimidazole. Throughout the years, the benzimidazole moiety has been used as a scaffold to synthesize a wide variety of compounds involved in biological processes; in the literature, many examples support the antioxidant properties and neuroprotective role of derivatives from this class [21,22]. Notably, **3** and **4** have similar motifs formed by two condensed rings bearing nitrogen atoms. The ethyl bridge was identified as an interesting molecular motif providing efficient ROS scavenging activity through Hydrogen Atom Transfer (HAT) when adjacent to aromatic or unsaturated moieties, which contribute to stabilizing the radical product [16–19]. Finally, the selenium atom was inserted in the system because of its proven capacity to reduce hydroperoxides [23] and its role in maintaining the human redox balance [24]. The presence of a selenium atom might improve the overall scavenging activity, as we previously observed in the case of **5** and its analog selenofluoxetine [19].

The synthetic scheme for the preparation of benzimidazolium salts is presented in Scheme 2. The benzimidazolium salts were synthesized by slightly modifying the procedures from the literature [25–29]. In more detail, benzimidazole was initially reacted with 1,2-dibromoethane in acetonitrile in the presence of K_2CO_3. The resulting intermediate **a** was treated with reduced diphenyl diselenide, which was prepared in situ by using $NaBH_4$, to provide compound **b**. This was refluxed in ethyl iodide to obtain **1**; the feasible quaternization of the N3 atom was proven, which also involved isolating the isopropyl derivative **2**, by refluxing **b** in isopropyl iodide.

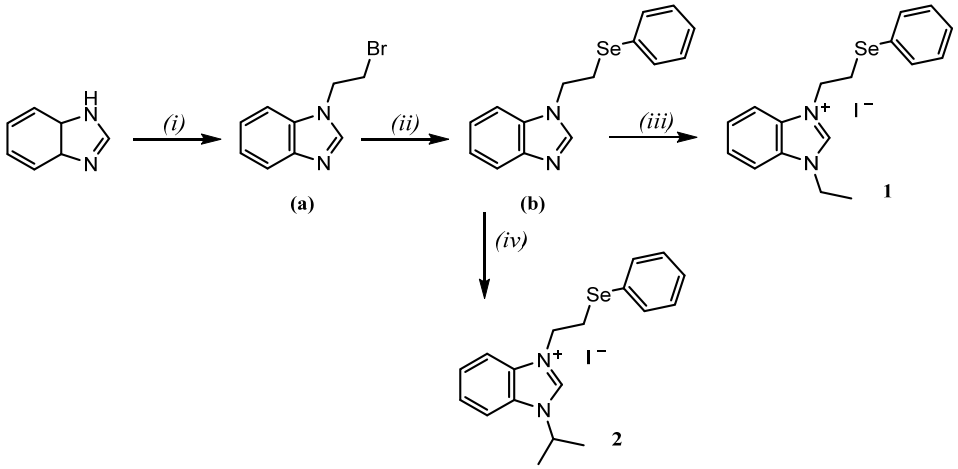

Scheme 2. Synthetic procedures for the preparation of compounds **a**, **b**, **1,** and **2**: (i) 1,2-dibromoethane, K_2CO_3, acetonitrile; (ii) diphenyl diselenide, $NaBH_4$, KI, ethanol; (iii) ethyl iodide, reflux; (iv) isopropyl iodide, reflux.

Final products were isolated via column chromatography and characterized to assess identity and purity profiles (see Supplementary Materials).

The physicochemical descriptors that can aid in defining organic compounds as drug-like molecules were computed for **1** and **2** [30,31]. Interestingly, ideal values for pharmacokinetic parameters including lipophilicity, size, polarity, solubility, unsaturation, and flexibility were predicted, supporting the drug-likeness of the synthesized compounds, as no violation was observed. In fact, according to this simulation, the compounds fall within the suitable physicochemical space for orally bioavailable compounds as the "Lipinski's rule of five" is fully respected [32]. Moreover, based on the computed physicochemical descriptors, and, in particular, on topological polar surface area (TPSA) and partition coefficient (logP) parameters which are stricter for CNS-targeting drugs [33,34], passive blood–brain barrier (BBB) permeation was predicted for these compounds. A TPSA value of 8.81 $Å^2$ was computed for both molecules, while logP values of 2.40 and 2.96 were estimated for **1** and **2**, respectively. For comparison, the same properties were computed for the reference compound zolpidem, obtaining TPSA and logP values of 37.61 $Å^2$ and of 3.25, respectively. Similarly, this compound is predicted to passively permeate through the BBB according to these values.

The synthesized molecules were designed with the aim of obtaining a higher antioxidant activity thanks to the introduction of the selenium center which enables additional antioxidant mechanisms.

In particular, the reactivity of alkyl selenides toward ROS has been described in the literature, and the subsequent oxidation and elimination reactions that such molecules undergo when inactivating oxidant species have been widely studied both experimentally and computationally [23,35]. In a previous work, our group investigated the mechanisms underlying the oxidation of phenyl alkyl selenides and the following selenoxide elimination in model substrates treated with H_2O_2 by using NMR, mass spectrometry, and density functional theory (DFT) [24]. Selenoxide elimination leads to the formation of selenenic acid and olefin [17], and this reaction has a biological relevance in the context of oxidative stress modulation [9,36], but also in the field of organic synthesis [24,37,38]. In particular, recent reports underline the relevance of the antioxidant properties and the capacity of detoxifying ROS in biological contexts of such molecules [39,40].

It must be anyway pointed out that the antioxidant features of the synthesized compounds should be further investigated by means of mechanistic studies to assess the contribution of the introduction of the selenium atom. Nevertheless, the selenium-based compounds should ideally also maintain their original pharmacological role, as we previously reported for selenofluoxetine [19]. Thus, to assess the potential binding motif of

the newly synthesized derivatives with the GABA A receptor, the target of zolpidem, we performed molecular modeling studies. In particular, molecular docking was enrolled to preliminarily investigate the interaction of the molecules with this target.

More specifically, the cryo-EM structure of the human GABA A receptor in complex with zolpidem was used (PDB ID 8DD2). This structure was deposited very recently, and it represents a valuable tool for studying the interaction of the zolpidem analog with this target [41]. In fact, the interaction of zolpidem with the GABA A receptor was previously studied through molecular docking. Various populations of orientations were detected, but the authors widely discussed the interaction pattern with the residues of the benzodiazepine binding site (site A) [42]. Then, cryo-EM data confirmed the calculations even if the cognate ligand was also retrieved in two other sites (sites B1 and B2, Figure 1) [41].

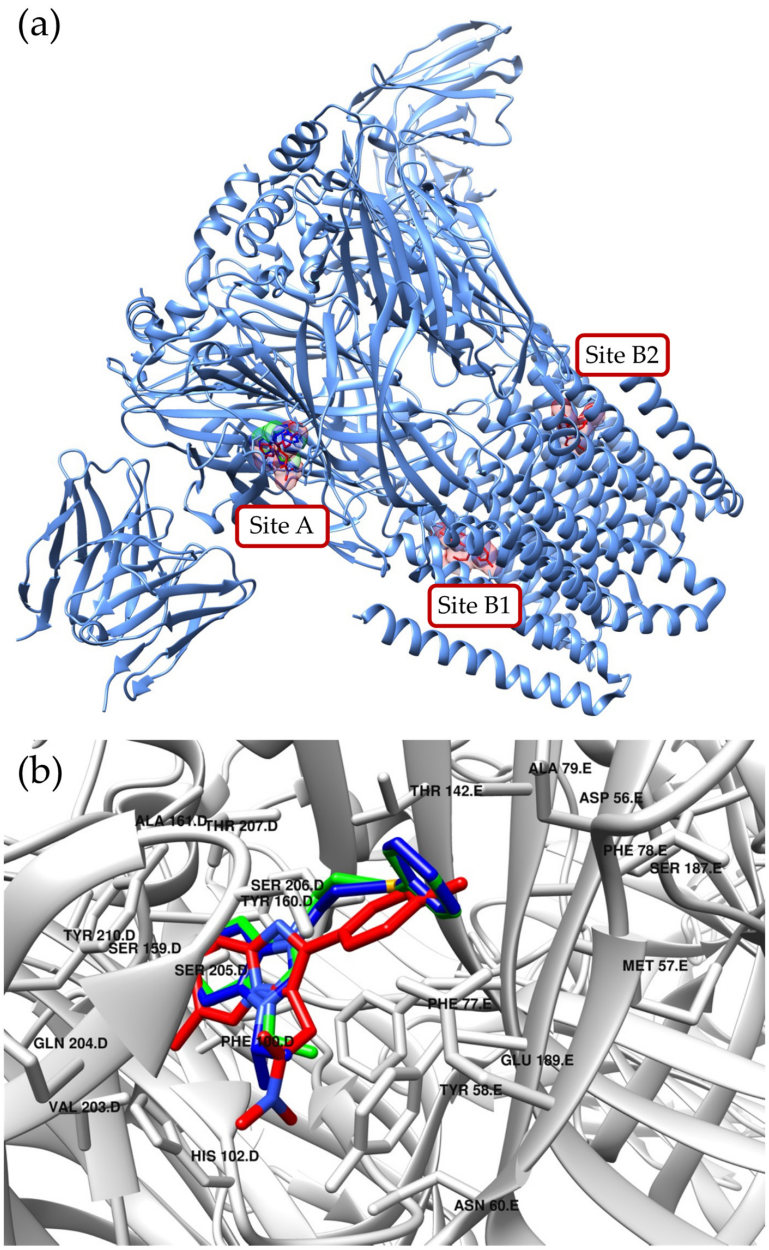

Figure 1. GABA A receptor in complex with zolpidem, which is depicted in red (PDB ID 8DD2). In the picture, the three binding sites identified for zolpidem by Cryo-EM have been labeled as site A, B1, and B2. The computed binding poses for compounds **1** and **2** in the benzodiazepine binding site (site A) are represented in green and blue, respectively (**a**). A magnification of site A is reported in panel (**b**) showing the interaction motif that was predicted for the compounds.

Thus, in the case of the current study, site-specific docking was performed by considering the biologically relevant benzodiazepine site, and the accuracy of the method was checked by re-docking the cognate ligand, which was fully superimposed onto the original pose. Compounds **1** and **2** fitted within the identified binding pocket that partially shared a similar interaction motif (Figure 1). Calculated binding energy values of −9.3 and −9.6 kcal mol^{-1} were computed for the two compounds. In Figure 1, the residues within interaction distance (<5 Å) have been labelled.

Importantly, this preliminary docking study demonstrated that the aromatic scaffolds of compounds **1** and **2** are fully superimposed onto that of the cognate ligand zolpidem in the benzodiazepine binding site of the GABA A receptor (site A). Additionally, the substituents show similar orientations, and the interaction motif with the residues of the macromolecular target is comparable to that shown by a parent drug.

It must be also pointed out that, according to Zhu et al. [41] zolpidem was also detected in two other sites in the synaptic side via cryo-EM analysis (sites B1 and B2, Figure 1), as anticipated above. These sites were defined by the authors as "approximately equivalent", and the functional role of the interaction of zolpidem with these regions remains unclear [41]. For comparison, docking was also performed to these two additional sites. In more detail, the docking of synthesized molecules to these sites showed less promising scores, with calculated binding energy values of −5.2 and −4.6 kcal mol^{-1} for compound **1** and of −5.3 and −5.4 kcal mol^{-1} for compound **2** in sites B1 and B2, respectively.

Overall, these simulations suggest that the activity on GABA A modulation may be maintained by the newly synthesized selenium-based compounds following their interaction with the benzodiazepine site (site A).

3. Materials and Methods

Commercially available chemicals were purchased from Sigma-Aldrich and used without any further purification. NMR experiments were performed on Bruker Avance III 400 and Bruker AMX 300 spectrometers (Bruker, Billerica, MA, USA). For data processing, TopSpin 4.1.4 and iNMR 6.4.5 (Nucleomatica, Molfetta, Italy) were used, and the spectra were calibrated by using solvent signal. Mass spectra were recorded via direct infusion electrospray (ESI) on an LCQ Fleet ion trap spectrometer (Thermo Scientific, Waltham, MA, USA). The purity profile was assayed via HPLC by using a Pro-Star system (Palo Alto, CA, USA) equipped with a 1706 UV-VIS detector (Bio-Rad, Hercules, CA, USA) and a C-18 column (5 µm, 4.6 × 150 mm) (Agilent, Santa Clara, CA, USA). An appropriate gradient of 0.1% formic acid (A) and acetonitrile (B) was used as a mobile phase with an overall flow rate of 1 mL min^{-1}. The general method for the analyses is reported in the following: 0 min (90% A−10% B), 2 min (90% A−10% B), 10 min (5% A−95% B), 14 min (5% A−95% B), and 16 min (90% A−10% B). Analyses were performed at 254 nm, and the purity profile was above 95% for final compounds (area %). Spectra and HPLC chromatograms are reported in the Supplementary Materials.

*3.1. Synthesis of 1-(2-Bromoethyl)-1H-benzo[d]imidazole (***a***)*

Benzimidazole (500 mg, 4.23 mmol) and K_2CO_3 (1.17 g, 8.46 mmol) were suspended in acetonitrile (20 mL). The reaction mixture was refluxed for 30 min. 1,2-dibromoethane (1.46 mL, 16.9 mmol) was then added to the reaction flask, and the mixture was refluxed for a further 3 h, while the reaction was monitored through TLC (DCM/MeOH 98:2). A further 4 equivalents of 1,2-dibromoethane were then added, and the heating was continued for another 48 h. The product was then extracted by using ethyl acetate (4 × 20 mL), and the organic layer was washed with water (2 × 20 mL). The organic phase was dried over sodium sulfate, and then the solvent was evaporated under reduced pressure to afford the final product as an orange oil. Yield: 42%. ^{1}H NMR ($CDCl_3$, 300 MHz) δ: 7.97 (1H, s, NCHN), 7.86 (1H, m, Ar), 7.81 (1H, m, Ar), 7.50 (1H, m, Ar), 7.27 (7H, m, Ar), 4.56 (2H, t,

J = 6.9 Hz, CH_2Br), 3.68 (2H, t, J = 6.9 Hz, CH_2). ESI-MS: m/z calculated for $C_9H_{10}BrN_2^+$: 225.00, found: 225.01 ($M+H^+$).

*3.2. Synthesis of 1-(2-(Phenylselanyl)ethyl)-1H-benzo[d]imidazole (**b**)*

Diphenyl diselenide (258 mg, 0.826 mmol) was dissolved in ethanol (20 mL). The solution was cooled to 0 °C by using an ice bath. $NaBH_4$ (95 mg, 2.51 mmol) was added to the flask while still in ice. The solution was left to be stirred for 15 min, and the yellow solution turned clear. Compound **a** (400 mg, 1.78 mmol) was added to the reaction mixture, which was then removed from ice and left to be stirred for 14 h. The reaction was monitored by using TLC (DCM/MeOH 98:2). A further 3 equivalents of $NaBH_4$ were added along with 2.2 equivalents of KI. The reaction mixture was left to be stirred overnight at room temperature. After completion, the mixture was poured in water (20 mL), and the product was extracted by using ethyl acetate (3 × 20 mL). Organic layers were combined, evaporated over sodium sulfate, and evaporated under reduced pressure, and the final product was obtained as a yellow oil. Yield: 95%. ^{1}H NMR ($CDCl_3$, 300 MHz) δ: 7.87 (1H, s, Ar), 7.80 (1H, m, Ar), 7.52 (1H, m, Ar), 7.28 (7H, m, Ar), 4.41 (2H, t, J = 7.2 Hz, NCH_2), 3.27 (2H, t, J = 7.2 Hz, CH_2Se). ESI-MS: m/z calculated for $C_{15}H_{15}N_2Se^+$: 303.04, found: 303.04 ($M+H^+$).

*3.3. Synthesis of 3-Ethyl-1-(2-(phenylselanyl)ethyl)-benzimidazolium Iodide (**1**)*

Ethyl iodide (3 mL, 37.3 mmol) was added to compound **b** (100 mg, 0.33 mmol), and the mixture was refluxed. The progress of the reaction was monitored through TLC (DCM/MeOH 98:2). After completion, unreacted ethyl iodide was evaporated under reduced pressure, and the obtained crude product was purified via column chromatography (from DCM/MeOH 98:2 to DCM/MeOH/TEA 93:5:2). The fractions containing the product were evaporated under reduced pressure, and the final product was obtained as a yellow solid. Yield: 61%. ^{1}H NMR ($CDCl_3$, 400 MHz) δ: 11.06 (1H, s, NCHN), 7.64 (4H, m, Ar), 7.34 (2H, m, Ar), 7.18 (3H, m, Ar), 4.97 (2H, t, J = 6.8 Hz, NCH_2), 4.52 (2H, q, J = 7.6 Hz, CH_2CH_3), 3.64 (2H, t, J = 6.8 Hz, CH_2Se), 1.72 (3H, t, J = 6.8 Hz, CH_3). ^{13}C NMR ($CDCl_3$, 100 MHz) δ: 141.5, 133.4, 131.7, 130.7, 130.0, 129.0, 127.3, 127.2, 126.7, 113.4, 112.9, 47.4, 43.1, 33.6, 14.7. ESI-MS: m/z calculated for $C_{17}H_{19}N_2Se^+$: 331.07, found: 331.28 (M^+).

*3.4. Synthesis of 3-Isopropyl-1-(2-(phenylselanyl)ethyl)-benzimidazolium Iodide (**2**)*

Isopropyl iodide (3 mL) was added to compound **b** (100 mg, 0.33 mmol), and the mixture was refluxed. The progress of the reaction was monitored through TLC (DCM/MeOH 98:2). After completion, unreacted isopropyl iodide was evaporated under reduced pressure, and the obtained crude product was purified via column chromatography (form DCM/MeOH 98:2 to DCM/MeOH/TEA 93:5:2). The fractions containing the product were evaporated under reduced pressure, and the final product was obtained as a brown solid. Yield: 64%. ^{1}H NMR ($CDCl_3$, 300 MHz) δ: 10.94 (1H, s, NCHN), 7.53 (4H, m, Ar), 7.21 (2H, m, Ar), 7.08 (3H, m, Ar), 4.94 (2H, t, J = 6.5 Hz, NCH_2), 4.77 (1H, m, J = 6.5 Hz, CH), 3.57 (2H, t, J = 6.5 Hz, CH_2Se), 1.70 (6H, d, J = 6.5 Hz, CH_3). ^{13}C NMR ($CDCl_3$, 100 MHz) δ: 143.9, 143.1, 133.9, 133.3, 126.6, 125.0, 123.0, 119.4, 119.1, 118.0, 105.0, 44.1, 40.0, 35.1, 28.2. ESI-MS: m/z calculated for $C_{18}H_{21}N_2Se^+$: 345.09, found: 345.32 (M^+).

3.5. Prediction of Physicochemical Descriptors

For compounds **1** and **2**, physicochemical descriptors relevant for drug-likeness, ADME parameters, and pharmacokinetic properties were computed by using the SwissADME tool (www.swissadme.ch, accessed on 11 May 2023, Molecular Modelling Group–Swiss Institute of Bioinformatics, Lausanne, Switzerland) [30,31].

3.6. Molecular Docking Studies

The 3D cryo-EM structure of Human GABA A receptor alpha1-beta2-gamma2 subtype in complex with the GABA A plus zolpidem was retrieved from the RCSB Protein Data Bank (www.rcsb.org, PDB ID 8DD2, resolution 2.90 Å) [41].

Prior to site-specific docking studies, the protein was prepared, and selected chains were isolated and considered. The ligand was built and prepared by using Avogadro [43]. The site-specific molecular docking study was performed by using AutoDock Vina [44,45]. The search volume for the benzodiazepine site (site A) was centered on the cognate ligand zolpidem and set according to the following parameters: x = 162.721, y = 109.298, z = 110.537; size: 35.000 × 35.000 × 35.000 Å. For the other two sites, the grid was again centered on the cognate ligand, and the following parameters were used: x = 111.601, y = 138.125, z = 105.358; size: 35.000 × 35.000 × 35.000 Å (site B1); x = 97.498, y = 123.997, z = 134.003; size: 35.000 × 35.000 × 35.000 Å (site B2). The docking simulation was carried out with default Vina parameters, the number of generated docking poses was set to 8, and the docking energy conformation value was expressed in −kcal/mol. The best scoring pose was selected for further analyses.

UCSF Chimera molecular viewer was used to produce the artworks [46].

4. Conclusions

This work aimed at the design and synthesis of compounds from a new class of derivatives that are structurally related to CNS-targeting agents and that bear a selenium nucleus. In particular, zolpidem and melatonin served as an inspiration to design the novel molecules, which were conceived also based on the results of our previous synthetic in silico and in vivo studies on selenofluoxetine.

Compounds **1** and **2** were obtained through a facile three-steps synthesis, and the molecules were predicted to efficiently cross BBB. Additionally, molecular docking studies showed that the compounds bind to the GABA A receptor, the macromolecular target of zolpidem, with a similar interaction motif with respect to the parent drug, suggesting that the action on CNS could be maintained by these new derivatives.

The designed pathway allows the production of several other potentially CNS-targeting derivatives through minor modifications of the scheme, allowing for future structure–activity relationship studies based on computational and in vitro reactivity tests.

Supplementary Materials: The following supporting information can be downloaded at: https://www.mdpi.com/article/10.3390/chemistry5030101/s1, Figure S1: ^{1}H-NMR of **1**; Figure S2: ^{13}C-NMR of **1**; Figure S3: ^{1}H-NMR of **2**; Figure S4: ESI-MS of **1**; Figure S5: ESI-MS of **2**; Figure S6: HPLC profiles of **1** (black) and **2** (red, 254 nm).

Author Contributions: Conceptualization, G.R., M.B., G.Z. and L.O.; methodology, G.R. and G.Z.; validation, G.R. and G.Z.; formal analysis, G.R., D.Z. and A.O.; investigation, G.R. and A.O.; resources, G.Z. and L.O.; data curation, G.R. and A.O.; writing—original draft preparation, G.R., D.Z., M.B. and L.O.; writing—review and editing, G.R. and L.O.; visualization, D.Z. and M.B.; supervision, G.R., G.Z. and L.O.; funding acquisition, L.O. All authors have read and agreed to the published version of the manuscript.

Funding: This research was funded by Università degli Studi di Brescia and Università degli Studi di Padova thanks to the P-DiSC (BIRD2018-UNIPD) project MAD3S (Modeling Antioxidant Drugs: Design and Development of computer-aided molecular Systems); P.I., L.O.

Data Availability Statement: The data is available within the article or its Supplementary Materials.

Conflicts of Interest: The authors declare no conflict of interest.

References

1. Sies, H. Oxidative Stress: A Concept in Redox Biology and Medicine. *Redox Biol.* **2015**, *4*, 180–183. [CrossRef]
2. Dubois-Deruy, E.; Peugnet, V.; Turkieh, A.; Pinet, F. Oxidative Stress in Cardiovascular Diseases. *Antioxidants* **2020**, *9*, 864. [CrossRef]

3. Klaunig, J.E. Oxidative Stress and Cancer. *Curr. Pharm. Des.* **2019**, *24*, 4771–4778. [CrossRef]
4. Barnham, K.J.; Masters, C.L.; Bush, A.I. Neurodegenerative Diseases and Oxidative Stress. *Nat. Rev. Drug Discov.* **2004**, *3*, 205–214. [CrossRef]
5. Tobe, E. Mitochondrial Dysfunction, Oxidative Stress, and Major Depressive Disorder. *Neuropsychiatr. Dis. Treat.* **2013**, *9*, 567–573. [CrossRef]
6. Emiliani, F.E.; Sedlak, T.W.; Sawa, A. Oxidative Stress and Schizophrenia. *Curr. Opin. Psychiatry* **2014**, *27*, 185–190. [CrossRef]
7. Eleutherio, E.C.A.; Silva Magalhães, R.S.; de Araújo Brasil, A.; Monteiro Neto, J.R.; de Holanda Paranhos, L. SOD1, More than Just an Antioxidant. *Arch. Biochem. Biophys.* **2021**, *697*, 108701. [CrossRef]
8. Flohé, L.; Toppo, S.; Orian, L. The Glutathione Peroxidase Family: Discoveries and Mechanism. *Free Radic. Biol. Med.* **2022**, *187*, 113–122. [CrossRef]
9. Orian, L.; Flohé, L. Selenium-Catalyzed Reduction of Hydroperoxides in Chemistry and Biology. *Antioxidants* **2021**, *10*, 1560. [CrossRef]
10. Deisseroth, A.; Dounce, A.L. Catalase: Physical and Chemical Properties, Mechanism of Catalysis, and Physiological Role. *Physiol. Rev.* **1970**, *50*, 319–375. [CrossRef]
11. Gassen, M.; Youdim, M.B.H. Free Radical Scavengers: Chemical Concepts and Clinical Relevance. *J. Neural Transm. Suppl.* **1999**, *56*, 193–210.
12. Brewer, M.S. Natural Antioxidants: Sources, Compounds, Mechanisms of Action, and Potential Applications. *Compr. Rev. Food Sci. Food Saf.* **2011**, *10*, 221–247. [CrossRef]
13. Marino, A.; Battaglini, M.; Moles, N.; Ciofani, G. Natural Antioxidant Compounds as Potential Pharmaceutical Tools against Neurodegenerative Diseases. *ACS Omega* **2022**, *7*, 25974–25990. [CrossRef]
14. Ribaudo, G.; Bortoli, M.; Pavan, C.; Zagotto, G.; Orian, L. Antioxidant Potential of Psychotropic Drugs: From Clinical Evidence to In Vitro and In Vivo Assessment and toward a New Challenge for in Silico Molecular Design. *Antioxidants* **2020**, *9*, 714. [CrossRef]
15. Zeppilli, D.; Ribaudo, G.; Pompermaier, N.; Madabeni, A.; Bortoli, M.; Orian, L. Radical Scavenging Potential of Ginkgolides and Bilobalide: Insight from Molecular Modeling. *Antioxidants* **2023**, *12*, 525. [CrossRef]
16. Bortoli, M.; Dalla Tiezza, M.; Muraro, C.; Pavan, C.; Ribaudo, G.; Rodighiero, A.; Tubaro, C.; Zagotto, G.; Orian, L. Psychiatric Disorders and Oxidative Injury: Antioxidant Effects of Zolpidem Therapy Disclosed In Silico. *Comput. Struct. Biotechnol. J.* **2019**, *17*, 311–318. [CrossRef]
17. Ribaudo, G.; Bortoli, M.; Ongaro, A.; Oselladore, E.; Gianoncelli, A.; Zagotto, G.; Orian, L. Fluoxetine Scaffold to Design Tandem Molecular Antioxidants and Green Catalysts. *RSC Adv.* **2020**, *10*, 18583–18593. [CrossRef]
18. Muraro, C.; Dalla Tiezza, M.; Pavan, C.; Ribaudo, G.; Zagotto, G.; Orian, L. Major Depressive Disorder and Oxidative Stress: In Silico Investigation of Fluoxetine Activity against ROS. *Appl. Sci.* **2019**, *9*, 3631. [CrossRef]
19. Ribaudo, G.; Bortoli, M.; Witt, C.E.; Parke, B.; Mena, S.; Oselladore, E.; Zagotto, G.; Hashemi, P.; Orian, L. ROS-Scavenging Selenofluoxetine Derivatives Inhibit In Vivo Serotonin Reuptake. *ACS Omega* **2022**, *7*, 8314–8322. [CrossRef]
20. Dalla Tiezza, M.; Ribaudo, G.; Orian, L. Organodiselenides: Organic Catalysis and Drug Design Learning from Glutathione Peroxidase. *Curr. Org. Chem.* **2019**, *23*, 1381–1402. [CrossRef]
21. Ullah, A.; Al Kury, L.T.; Althobaiti, Y.S.; Ali, T.; Shah, F.A. Benzimidazole Derivatives as New Potential NLRP3 Inflammasome Inhibitors That Provide Neuroprotection in a Rodent Model of Neurodegeneration and Memory Impairment. *J. Inflamm. Res.* **2022**, *15*, 3873–3890. [CrossRef]
22. Aleyasin, H.; Karuppagounder, S.S.; Kumar, A.; Sleiman, S.; Basso, M.; Ma, T.; Siddiq, A.; Chinta, S.J.; Brochier, C.; Langley, B.; et al. Antihelminthic Benzimidazoles Are Novel HIF Activators That Prevent Oxidative Neuronal Death via Binding to Tubulin. *Antioxid. Redox Signal.* **2015**, *22*, 121–134. [CrossRef]
23. Ribaudo, G.; Bellanda, M.; Menegazzo, I.; Wolters, L.P.; Bortoli, M.; Ferrer-Sueta, G.; Zagotto, G.; Orian, L. Mechanistic Insight into the Oxidation of Organic Phenylselenides by H_2O_2. *Chem. Eur. J.* **2017**, *23*, 2405–2422. [CrossRef]
24. Ribaudo, G.; Bortoli, M.; Oselladore, E.; Ongaro, A.; Gianoncelli, A.; Zagotto, G.; Orian, L. Selenoxide Elimination Triggers Enamine Hydrolysis to Primary and Secondary Amines: A Combined Experimental and Theoretical Investigation. *Molecules* **2021**, *26*, 2770. [CrossRef]
25. Dubey, P.; Singh, A.K. Sonogashira Coupling (Cu/Amine-Free) of ArBr/Cl in Aerobic Condition and N—Benzylation of Aniline with Benzyl Alcohol Catalyzed by Complexes of Pd(II) with Sulfated/Selenated NHCs. *ChemistrySelect* **2020**, *5*, 2925–2934. [CrossRef]
26. Dubey, P.; Gupta, S.; Singh, A.K. Trinuclear Complexes of Palladium(II) with Chalcogenated N-Heterocyclic Carbenes: Catalysis of Selective Nitrile–Primary Amide Interconversion and Sonogashira Coupling. *Dalton Trans.* **2017**, *46*, 13065–13076. [CrossRef]
27. Khandaka, H.; Kumar Joshi, R. Fe3O4@SiO2Supported Pd (II)-Selenoether N-Heterocyclic Carbene: A Highly Active and Reusable Heterogeneous Catalyst for C O Cross-Coupling of Alcohols and Chloroarenes. *Tetrahedron Lett.* **2022**, *111*, 154163. [CrossRef]
28. Kumari, S.; Sharma, C.; Satrawala, N.; Srivastava, A.K.; Sharma, K.N.; Joshi, R.K. Selenium-Directed *Ortho* C–H Activation of Benzyl Selenide by a Selenated NHC–Half-Pincer Ruthenium(II) Complex. *Organometallics* **2022**, *41*, 1403–1411. [CrossRef]
29. Sharma, K.N.; Satrawala, N.; Srivastava, A.K.; Ali, M.; Joshi, R.K. Palladium(II) Ligated with a Selenated (Se, C_{NHC}, N^-)-Type Pincer Ligand: An Efficient Catalyst for Mizoroki–Heck and Suzuki–Miyaura Coupling in Water. *Org. Biomol. Chem.* **2019**, *17*, 8969–8976. [CrossRef]

30. Daina, A.; Zoete, V. A BOILED-Egg To Predict Gastrointestinal Absorption and Brain Penetration of Small Molecules. *ChemMedChem* **2016**, *11*, 1117–1121. [CrossRef]
31. Daina, A.; Michielin, O.; Zoete, V. SwissADME: A Free Web Tool to Evaluate Pharmacokinetics, Drug-Likeness and Medicinal Chemistry Friendliness of Small Molecules. *Sci. Rep.* **2017**, *7*, 42717. [CrossRef]
32. Lipinski, C.A.; Lombardo, F.; Dominy, B.W.; Feeney, P.J. Experimental and Computational Approaches to Estimate Solubility and Permeability in Drug Discovery and Development Settings. *Adv. Drug Deliv. Rev.* **2001**, *46*, 3–26. [CrossRef]
33. Pajouhesh, H.; Lenz, G.R. Medicinal Chemical Properties of Successful Central Nervous System Drugs. *NeuroRX* **2005**, *2*, 541–553. [CrossRef]
34. Wager, T.T.; Chandrasekaran, R.Y.; Hou, X.; Troutman, M.D.; Verhoest, P.R.; Villalobos, A.; Will, Y. Defining Desirable Central Nervous System Drug Space through the Alignment of Molecular Properties, in Vitro ADME, and Safety Attributes. *ACS Chem. Neurosci.* **2010**, *1*, 420–434. [CrossRef]
35. Madabeni, A.; Zucchelli, S.; Nogara, P.A.; Rocha, J.B.T.; Orian, L. In the Chalcogenoxide Elimination Panorama: Systematic Insight into a Key Reaction. *J. Org. Chem.* **2022**, *87*, 11766–11775. [CrossRef]
36. Sun, C.; Wang, L.; Xianyu, B.; Li, T.; Gao, S.; Xu, H. Selenoxide Elimination Manipulate the Oxidative Stress to Improve the Antitumor Efficacy. *Biomaterials* **2019**, *225*, 119514. [CrossRef]
37. Macdougall, P.E.; Smith, N.A.; Schiesser, C.H. Substituent Effects in Selenoxide Elimination Chemistry. *Tetrahedron* **2008**, *64*, 2824–2831. [CrossRef]
38. Reich, H.J.; Wollowitz, S. Preparation of α,β-Unsaturated Carbonyl Compounds and Nitriles by Selenoxide Elimination. In *Organic Reactions*; John Wiley & Sons, Inc.: Hoboken, NJ, USA, 1993; pp. 1–296.
39. Sands, K.N.; Burman, A.L.; Ansah-Asamoah, E.; Back, T.G. Chemistry Related to the Catalytic Cycle of the Antioxidant Ebselen. *Molecules* **2023**, *28*, 3732. [CrossRef]
40. Mamgain, R.; Kostic, M.; Singh, F.V. Synthesis and Antioxidant Properties of Organoselenium Compounds. *Curr. Med. Chem.* **2023**, *30*, 2421–2448. [CrossRef]
41. Zhu, S.; Sridhar, A.; Teng, J.; Howard, R.J.; Lindahl, E.; Hibbs, R.E. Structural and Dynamic Mechanisms of $GABA_A$ Receptor Modulators with Opposing Activities. *Nat. Commun.* **2022**, *13*, 4582. [CrossRef]
42. Hanson, S.M.; Morlock, E.V.; Satyshur, K.A.; Czajkowski, C. Structural Requirements for Eszopiclone and Zolpidem Binding to the γ-Aminobutyric Acid Type-A ($GABA_A$) Receptor Are Different. *J. Med. Chem.* **2008**, *51*, 7243–7252. [CrossRef]
43. Hanwell, M.D.; Curtis, D.E.; Lonie, D.C.; Vandermeersch, T.; Zurek, E.; Hutchison, G.R. Avogadro: An Advanced Semantic Chemical Editor, Visualization, and Analysis Platform. *J. Cheminform.* **2012**, *4*, 17. [CrossRef]
44. Trott, O.; Olson, A.J. AutoDock Vina: Improving the Speed and Accuracy of Docking with a New Scoring Function, Efficient Optimization, and Multithreading. *J. Comput. Chem.* **2009**, *31*, 455–461. [CrossRef]
45. Eberhardt, J.; Santos-Martins, D.; Tillack, A.F.; Forli, S. AutoDock Vina 1.2.0: New Docking Methods, Expanded Force Field, and Python Bindings. *J. Chem. Inf. Model.* **2021**, *61*, 3891–3898. [CrossRef]
46. Pettersen, E.F.; Goddard, T.D.; Huang, C.C.; Couch, G.S.; Greenblatt, D.M.; Meng, E.C.; Ferrin, T.E. UCSF Chimera? A Visualization System for Exploratory Research and Analysis. *J. Comput. Chem.* **2004**, *25*, 1605–1612. [CrossRef]